AER/AGS Open File Report 2023-04

Earthquake Iso-Nuisance and Iso-Damage Mapping for Alberta: Preliminary Results

AER/AGS Open File Report 2023-04

Earthquake Iso-Nuisance and Iso-Damage Mapping for Alberta: Preliminary Results

M. Reyes Canales, E.J. Galloway, S.M. Pawley, J.A. Yusifbayov and G.M.D. Hartman

Alberta Energy Regulator
Alberta Geological Survey

January 2024

ISBN 978-1-4601-5710-7

If you use information from this publication in other publications or presentations, please acknowledge the AER/AGS. We recommend the following reference format:

Reyes Canales, M., Galloway, E.J., Pawley, S.M., Yusifbayov, J.A. and Hartman, G.M.D. (2024): Earthquake iso-nuisance and iso-damage mapping for Alberta: preliminary results; Alberta Energy Regulator / Alberta Geological Survey, AER/AGS Open File Report 2023-04, 11 p.

Publications in this series have undergone only limited review and are released essentially as submitted by the author.

Published January 2024 by:
Alberta Energy Regulator
Alberta Geological Survey
4th Floor, Twin Atria Building
4999 – 98th Avenue
Edmonton, AB T6B 2X3
Canada

Tel: 780.638.4491
Email: AGS-Info@aer.ca
Website: ags.aer.ca

Contents

Figures

Acknowledgements

The authors would like to thank Alex MacNeil, Todd Shipman, Chris Filewich, Matt Grobe, Kelsey MacCormack, and Andrew Beaton for their constructive and helpful support developing this project.

Abstract

Preliminary earthquake iso-nuisance and iso-damage maps for Alberta have been generated using three levels of nuisance and damage: (1) 50% probability of causing nuisance to 30 000 households and damage to 3 households; (2) 50% probability of causing nuisance to 20 000 households and damage to 2 households; (3) 50% probability to cause nuisance to 10 000 households and damage to 1 household. These maps show the earthquake magnitudes necessary at any given location in Alberta to achieve a particular threshold of nuisance and damage, considering human exposure factors and surficial geological conditions. For the human exposure factor, we depended on population distribution; for the surficial geological conditions, we utilized site amplification effects derived from estimates of the time-averaged shear-wave velocity to a depth of 30 m (Vs30) from surficial geological modelling. Earthquake iso-nuisance and iso-damage maps can provide valuable assistance in effectively managing current and future cases of induced seismicity in Alberta. They provide an overview of the impact of a wide range of earthquake scenarios and can function as the base to guide the development of red-light maps for different types of industrial activities once the appropriate trailing seismicity factor is defined for a given activity.

1 Introduction

The seismic hazard in areas with historically low seismicity in Alberta has risen due to induced seismicity events associated with industrial activity (Atkinson et al., 2016; Reyes Canales et al., 2022). To better understand the potential impact of future induced seismicity events, we developed earthquake iso-nuisance and iso-damage maps for Alberta. These maps show the earthquake magnitude required at any given location in Alberta to reach a specific level of nuisance and damage. In this context, the level of nuisance and damage refers to the probability of causing a certain nuisance or damage intensity to a given number of households (for instance, 50% probability of causing nuisance to 30 000 households, and damage to 3 households). The combination iso-risk map results from the merger of the iso-nuisance and iso-damage maps, and ultimately provides the base for the development of red-light maps in the management of induced seismicity. As a first approach, the estimations of nuisance and damage rely on modelling of the time-averaged shear-wave velocity to a depth of 30 m (Vs30) for the seismic site amplification, and on population distribution for the human exposure variable. In this initial approach, we do not include advanced frameworks for assessing human exposure variables, such as incorporating risk analysis of critical infrastructure.

In response to the rising seismic hazard from induced seismicity, the Alberta Energy Regulator has enforced regulations in specific regions, including three subsurface orders for hydraulic-fracturing activities: Subsurface Order No. 2 (SSO2, Alberta Energy Regulator, 2015), Subsurface Order No. 6 (SSO6, Alberta Energy Regulator, 2019), and Subsurface Order No. 7 (SSO7, Alberta Energy Regulator, 2019). Under these subsurface orders, operators must monitor the adjacent seismic events and follow a traffic light protocol. If a red-light event occurs (an event larger than a specific magnitude), the operators must immediately stop the hydraulic-fracturing activities. In the case of disposal activities, for instance, an Environmental Protection Order has been issued for the seismic activity east of Musreau Lake (Alberta Energy Regulator, 2021). Under this order, disposal operators must maintain a local passive seismic monitoring array to detect adjacent seismic events and develop a mitigation plan to reduce the magnitude and frequency of the seismic events.

Developing earthquake iso-nuisance and iso-damage maps can be beneficial in managing induced seismicity, since they provide an overview of the impact of a wide range of earthquake magnitudes considering key factors like seismic site amplification and human exposure. They can work as the base for future maps that can define red-light events, i.e., earthquakes from industrial activity that generate unacceptable ground motions.

2 Data and Methods

We implemented a similar methodology to that proposed by Schultz et al. (2021a, b) to develop earthquake iso-nuisance and iso-damage maps for Alberta. In the following section, we list the main steps to generate earthquake iso-nuisance and iso-damage maps:

1) **Generate Vs30 and population density maps**: A time-averaged shear wave velocity for the upper 30 m below the land surface (Vs30, Holzer et al., 2005) was created for Alberta based on compiled shear wave velocity values for different bedrock and surficial lithological units. Preference was given to studies reporting Vs30 values in the Western Canada Sedimentary Basin, although information from other regions was also used to complete the dataset. The mean and standard deviation of these compiled values was regionalized for bedrock units by relating the velocities to the dominant lithological composition indicated in the provincial-scale (1:1 000 000) Bedrock Geology of Alberta (Prior et al., 2013). For surficial units, a property model of sediments above bedrock (Pawley et al., 2023) was used to estimate the portion of coarse- and fine-grained surficial units in the upper 30 m, and the averaged velocities for clay-and sand-dominated units were associated with the model. For regions outside the province, Vs30 was determined through estimations of topographic slope (Heath et al., 2020). For population distribution, we utilized the LandScan 2020 global population database (Rose et al., 2021), which provides population data per square kilometre. We modified this population data to align with the impact cell size specified in this study (3 km by 3 km).
2) **Define Impact and earthquake node grids:** The impact grids contain information about population density and Vs30. The earthquake nodes define locations of synthetic earthquakes. For this study, we defined an impact grid size of 3 km by 3 km, and an earthquake node spacing of 10 km by 10 km, as applied by Schultz et al. (2021a, b).
3) **Generate synthetic earthquakes**: For each earthquake node, a range of synthetic earthquakes was defined (magnitudes and depths) for a single realization. In this analysis, we simulated 100 realizations per earthquake node, each realization containing events in a magnitude range between magnitudes M=2 to M=5. Impact cells up to 400 km and 40 km from the earthquake location were considered for the nuisance and damage calculations, respectively. We considered an earthquake depth distribution of 2, 5, and 7 km, with weights of 0.3, 0.5, and 0.2, respectively. Though relatively shallow in the wider seismological perspective, this distribution approximates the depth of the earthquakes induced in Alberta.
4) **Generate synthetic ground motion catalogs**: Given the distance and the earthquake magnitude, we relied on ground motion prediction equations (GMPEs) to estimate the corresponding ground motion (peak ground acceleration, PGA, and peak ground velocity, PGV) at each impact cell. The GMPEs were calibrated according to the site amplification conditions (Vs30), where lower Vs30 values lead to higher site amplification effects (ground motions). We included perturbation (aleatory uncertainty) for the ground motions, the Vs30, and population data. We used the GMPEs defined by Schultz and Nanometrics (2019) in this example.
5) **Calculate nuisance and damage**: The probability of nuisance and damage for a simulated earthquake was estimated using nuisance and fragility (damage) functions. In other words, for a given ground motion value in an impact cell, we estimated the probability of nuisance and damage per household. For nuisance functions, see Schultz et al. (2021c), and for fragility functions, see FEMA (2015). In this analysis, we used a community decimal intensity (CDI) of 3 for the nuisance, equivalent to a perceived “light shaking”. For the damage, we used a damage state (DS) of 1, which is equivalent to cosmetic damage in zones with low seismic hazard.
6) **Generate nuisance and damage curves:** From population distribution and the probabilities of nuisance/fragility per impact cell, we estimated the total number of households affected per simulated earthquake. Plots of the number of households affected vs. the earthquake magnitude are known as the nuisance and damage plots. Because of the multiple realizations (diverse realizations given by the perturbations and variabilities in the setting), there is a distribution of households affected per magnitude. The median of the distributions represents the 50% probability of households affected,

and we refer to it as the median curve for nuisance and damage plots. Nuisance and damage curves were calculated for each earthquake node.

7) **Generate iso-nuisance, iso-damage and combination iso-risk maps**: Given nuisance and damage tolerance thresholds, iso-nuisance and iso-damage maps were created (For instance, 50% probability of causing nuisance to 30 000 households, and damage to 3 households). For a given earthquake node, the nuisance curves were used to determine the earthquake magnitude that causes nuisance at the threshold level. This determination was performed using the same nuisance threshold for all nodes and the results are presented as an iso-nuisance map. An iso-damage map is created in a similar fashion using a damage tolerance threshold. Finally, a combination map resulted from choosing the lowest magnitude value from the iso-nuisance and iso-damage maps at each earthquake node location.

There are some differences to the methodology used by Schultz et al. (2021a, b). First, the earthquake nodes extend beyond the limits of a particular hydrocarbon resource play, and the depth of the synthetic earthquakes is independent of the depth of the resource play. Second, the earthquake iso-nuisance and iso-damage maps do not include trailing seismicity simulation from hydraulic fracturing activities. Thus, these maps show the actual spatial distribution of earthquake magnitude required to reach a specific level of nuisance and damage, and not directly the red-light earthquake magnitudes as shown by Schultz et al. (2021a, b). The rationale for excluding trailing seismicity is that these iso-nuisance and iso-damage maps can work as the base for future red-light maps for different types of industrial activities in Alberta, not only hydraulic-fracturing. Once the appropriate trailing seismicity factor is defined for a given activity and location, this can be incorporated to define a red-light map.

3 Results

3.1 Site Amplification Maps: Vs30 from Geological Information

Figure 1 shows the mean Vs30 (a) and population distribution (b) maps for Alberta and neighbouring areas used in this study. As explained before, for the regions within the province, Vs30 estimates rely on surficial geological modelling, while for regions outside the province, Vs30 values are determined by using topographic slope estimates in Alberta (Heath et al., 2020). For reference, Vs30=760 m/s is the boundary between B/C site conditions, which correspond to very dense soil and soft rock to rock (Canadian Commission on Building and Fire Codes, 2015). The mean Vs30 values in Figure 1a show a trend of increasing values towards the stable craton (northeast) and the Rocky Mountains (southeast). This is expected given the presence of hard rocks (igneous and metamorphic rocks) at the land surface in these regions, which increases the estimation of Vs30 values from surficial geological analysis (mean Vs30>1000 m/s). In contrast, we found lower mean Vs30 values towards the east (mean Vs30 values ranging between 500 and 900 m/s), where increasing site-amplification effects are expected given the dominance of soft sedimentary rocks and soils. For the population distribution map, we observe the highest concentration in the south and central areas of the province, particularly the Edmonton-Calgary corridor, whereas large areas in the north are sparsely populated. To better appreciate the changes in the population distribution, the population information (Figure 1b) is shown using a logarithmic scale base 10 ranging from 0 to 10 000 people (equivalent to 0 to 4 in the logarithmic scale, respectively). For instance, a value of 1 equals 10 people per km^2, and a value of 3 equals 1000 people per km^2.

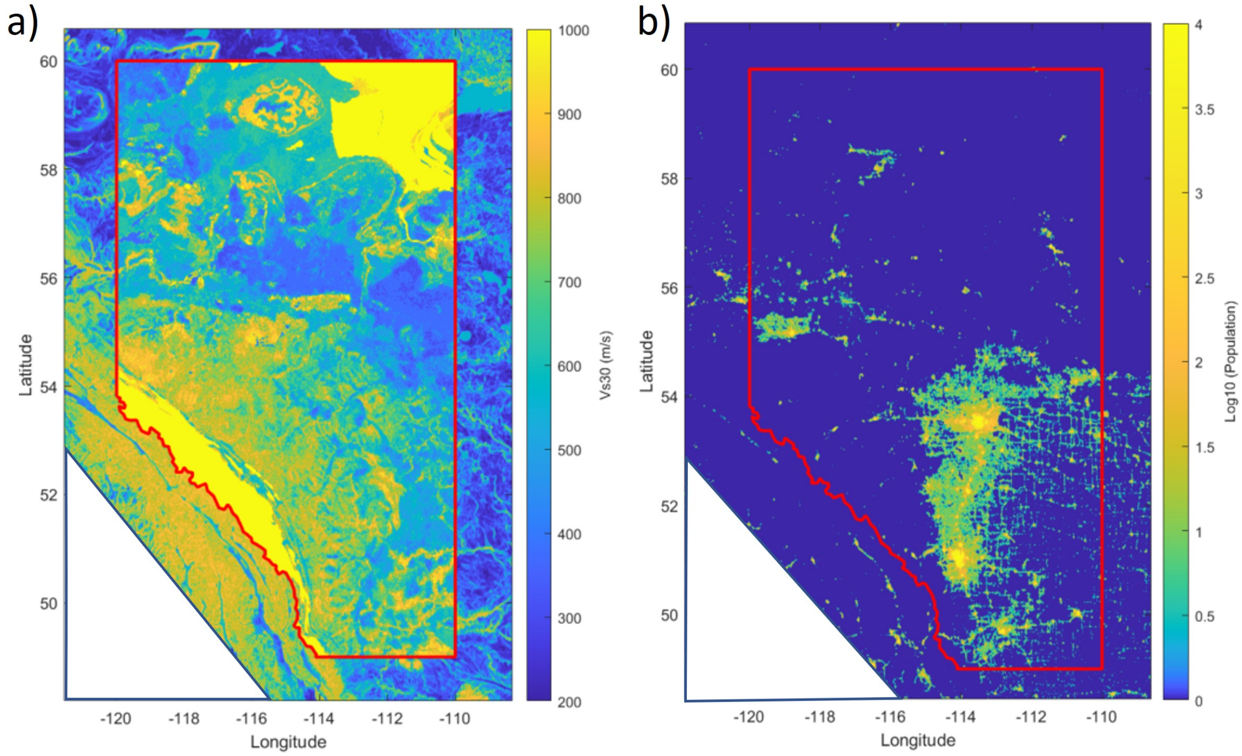

Figure 1. Mean Vs30 (a) and population distribution (b) maps for Alberta and neighbouring areas. Vs30 values for areas within Alberta are estimated using surficial geology information, whereas for regions located outside of the province, Vs30 is determined based on estimations of topographic slope (Heath et al., 2020). We employ the high-resolution global population dataset from Rose et al. (2021) to represent the distribution of population. The population information is shown using a logarithmic scale base 10.

3.2 Earthquake Iso-Nuisance, Iso-Damage and Combination Iso-Risk Maps for Alberta

The workflow outlined in the preceding section was applied to generate iso-nuisance, iso-damage, and combination iso-risk maps for the province of Alberta. Figures 2, 3, and 4 show the iso-nuisance, iso-damage, and combination iso-risk maps for Alberta using different tolerance levels: 50% probability of causing nuisance to 30 000 households, and damage to 3 households (Figure 2); 50% probability of causing nuisance to 20 000 households, and damage to 2 households (Figure 3); 50% probability of causing nuisance to 10 000 households, and damage to 1 household (Figure 4). In all cases, we refer to a nuisance equivalent to light-perceived shaking (CDI=3) and damage equivalent to slight/minor cosmetic damage (DS=1) for a construction that follows the building code standards in a low seismic hazard zone. For graphic purposes, the iso-nuisance maps were smoothed using a local median filter, remarking on the general trend of values.

These maps show the spatial distribution of earthquake magnitude required to reach a specific level of nuisance and damage. If an earthquake of magnitude M=3 occurs at shallow depth between 2 and 7 km in population centers like Edmonton or Calgary, there is a 50% probability of it causing nuisance to 30 000 households (CDI=3). Conversely, to achieve an equivalent level of nuisance in sparsely populated areas to the north, a seismic event with a magnitude greater than M=5 is necessary. As expected, the magnitude values decrease when a lower tolerance level is chosen. The average magnitude from the SSO2 area equals M=4.6, M=4.3, and M=4.1, given the combination iso-risk maps in Figures 2, 3, and 4, respectively. On the other hand, the red-light threshold for earthquakes in SSO2 equals M=4, similar to the average magnitude in the SSO2 area from Figure 4. However, the combination iso-risk maps should not be used as red-light maps for hydraulic fracturing, because we did not include a trailing seismicity factor in their generation.

We also noticed a marked contrast in magnitude values between more populated areas and less populated areas. For instance, the magnitude from the combination iso-risk map in Figure 4 (50% probability of causing nuisance to 10 000 households and damage to 1 household) values drop to magnitudes close to M=2.5 in largely populated centers like Edmonton and Calgary. In contrast, the magnitude values increase to M=5 in less populated areas like the north of the province. It should be noted that we account for both site amplification effects and population in the generation of the maps. However, the results of nuisance and damage from this initial setting seem to be mostly driven by the population distribution.

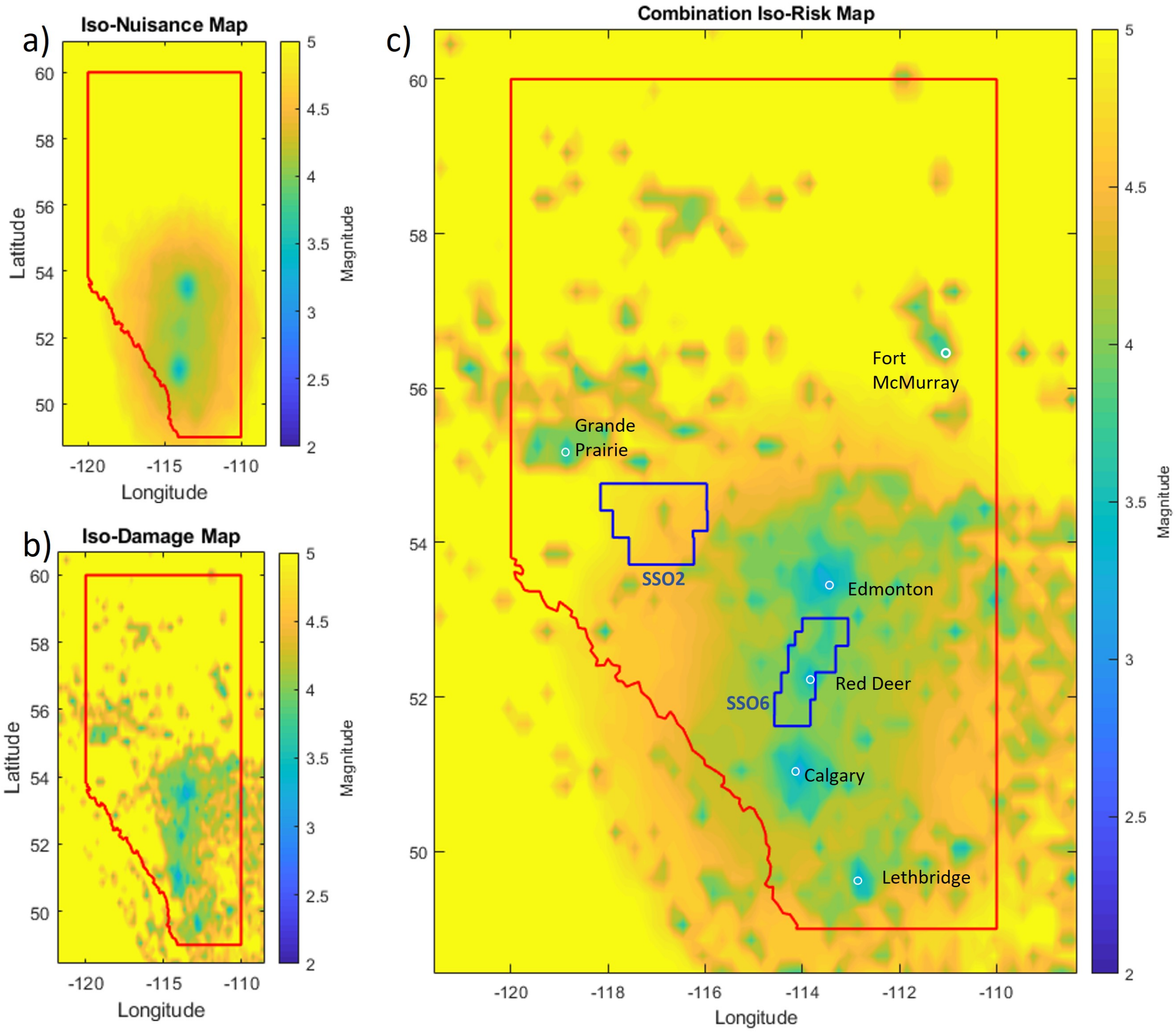

Figure 2. (a) Iso-nuisance map, using equivalent magnitudes for a tolerance level of 50% probability to cause nuisance to 30 000 households (CDI=3, equivalent to light-perceived shaking). (b) Iso-damage map, using equivalent magnitudes for a tolerance level of 50% probability to damage 3 households (DS=1, equivalent to slight/minor cosmetic damage). (c) Combination iso-risk map, created by merging of the iso-nuisance (50% probability to cause nuisance to 30 000 households) and iso-damage maps (50% probability to damage 3 households). For reference, the figure shows the areas specified by SSO2 and SSO6.

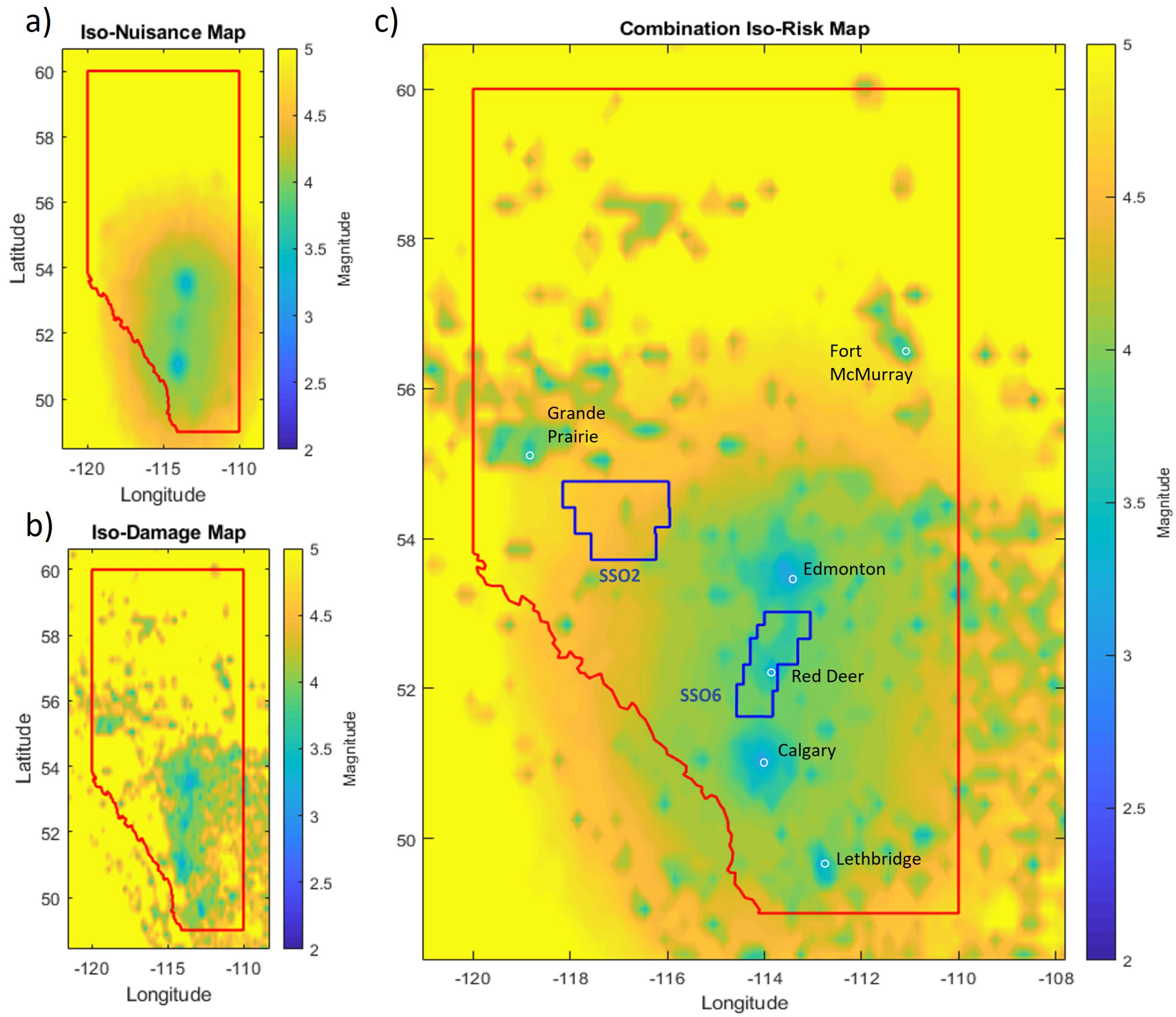

Figure 3. (a) Iso-nuisance map, using equivalent magnitudes for a tolerance level of 50% probability to cause nuisance to 20 000 households (CDI=3, equivalent to light-perceived shaking). (b) Iso-damage map, using equivalent magnitudes for a tolerance level of 50% probability to damage 2 households (DS=1, equivalent to slight/minor cosmetic damage). (c) Combination iso-risk map, created by merging of the iso-nuisance (50% probability to cause nuisance to 20 000 households) and iso-damage maps (50% probability to damage 2 households). For reference, the figure shows the areas specified by SSO2 and SSO6.

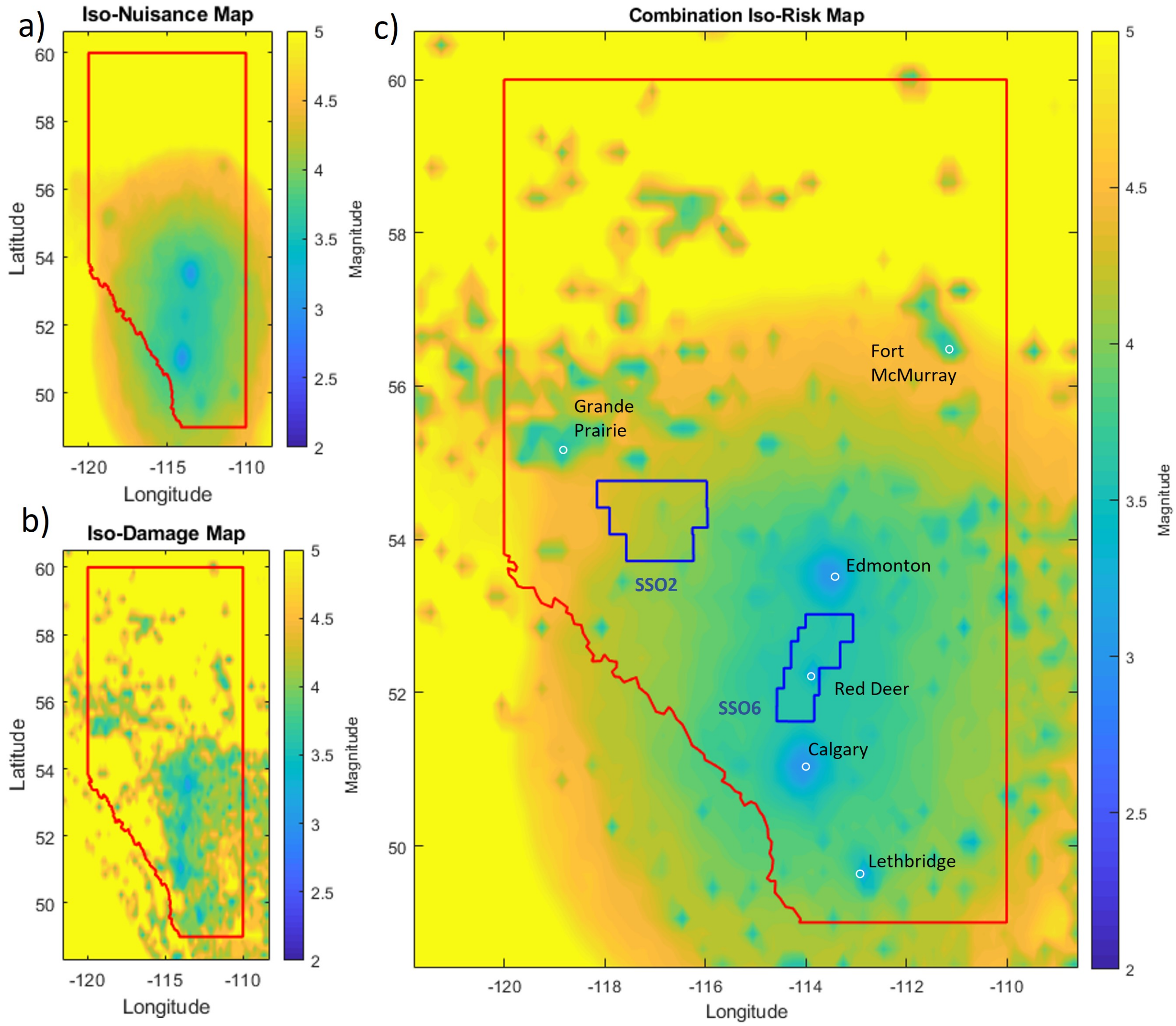

Figure 4. (a) Iso-nuisance map, using equivalent magnitudes for a tolerance level of 50% probability to cause nuisance to 10 000 households (CDI=3, equivalent to light-perceived shaking). (b) Iso-damage map, using equivalent magnitudes for a tolerance level of 50% probability to damage 1 household (DS=1, equivalent to slight/minor cosmetic damage). (c) Combination iso-risk map, merging of the iso-nuisance (50% probability to cause nuisance to 10 000 households) and iso-damage maps (50% probability to damage 1 household). For reference, the figure shows the areas specified by SSO2 and SSO6.

4 Discussion

These preliminary earthquake iso-nuisance and iso-damage maps are useful for managing induced seismicity since they provide insight into the impact of a range of earthquake magnitudes considering key factors like seismic site amplification and human exposure. However, these maps should not be used directly for setting traffic light protocol thresholds, but as the base for future red-light maps for different types of industrial activities in Alberta. To properly delineate maps applicable to traffic light protocols (red-light maps), a trailing seismicity factor should be included:

$$M_{red} = M_{limit} - dM_{trailing} \quad (1)$$

where M_{limit} refers to the magnitude indicated by the iso-nuisance and iso-damage maps at a particular tolerance level (e.g., 50% probability that 30 000 households are going the experience nuisance at a level of CDI=3, and 50% probability of causing damage to 3 households at a level of DS=1), $dM_{trailing}$ refers to the factor associated with the trailing seismicity since it is possible that an event larger than the earthquake that triggers the red light occurs after drastic operational changes (including stopping the operations), and M_{red} refers to the red-light magnitude that corresponds to a particular tolerance level.

In their analysis of red-light magnitudes from hydraulic-fracturing activities in different shale plays in North America, Schultz et al. (2021a, b) simulate a trailing seismicity factor for each earthquake magnitude. In areas like SSO2, we estimate that the simulation of trailing seismicity from Schultz et al. (2021b) leads to a trailing seismicity factor of $dM_{trailing} \simeq 0.5$. Therefore, if we subtract this factor from the magnitude values from a combination iso-risk map, given a particular tolerance level, we can delineate red-light maps from hydraulic fracturing activities. For instance, Figure 5a shows the combination iso-risk map for the SSO2 area, using a tolerance level of 50% probability of causing nuisance to 30 000 households, and damaging 3 households. Figure 5b shows the resulting magnitude map by subtracting a trailing seismicity factor of $dM_{trailing} \simeq 0.5$. By incorporating this factor, the values of Figure 5b can be interpreted as a red-light magnitude map for hydraulic-fracturing activities in the SSO2 area. Part of the reason why we chose a tolerance level similar to the one proposed by Schultz et al. (2021b) in the SSO2 area (i.e., 50% probability of causing nuisance to 30 000 households and damage to 3 households) is that the average magnitudes in SSO2 from Figure 5b equal M_{red}=4.1, which is similar to the current red-light magnitudes for the area (M_{red}=4.0).

The trailing seismicity factor, a key factor in determining the appropriate red-light magnitude, ultimately depends on the risk tolerance for seismicity following a significant event which led to drastic operation changes or stop of the activity (trailing seismicity after a red-light event). The same should be said about the magnitude M_{limit} which depends on the levels of nuisance and damage to be tolerated. Furthermore, other factors beyond the population distribution might be considered, such as critical infrastructure, warranting a different risk threshold. It should be noted that the described setting for red-light magnitude estimation is solely based on cases of induced seismicity from hydraulic fracturing. Other types of operations might require further adjustments in the trailing seismicity estimation or even a different approach for risk management. For instance, choosing the trailing seismicity factor for operations like subsurface disposal can be challenging due to the limited number of studies conducted to characterize the post-operational seismicity related to disposal activities in Alberta, particularly after a significant event (red-light). An example is the seismic cluster related to disposal activity east of Musreau Lake, which is still ongoing, though the operators are ordered to monitor and mitigate the seismicity. This contrasts with hydraulic-fracturing activities in Alberta, with multiple examples of concluding operations and detailed post-operational seismicity analysis in the literature (e.g., Schultz et al., 2021 b). Furthermore, trailing seismicity might last longer for long-term injections, warranting more conservative estimations for the trailing seismicity factor. Nevertheless, these maps including the trailing seismicity factor can certainly provide a guide, if not a red-light magnitude estimation, of what is considered acceptable in terms of nuisance and damage from induced seismicity.

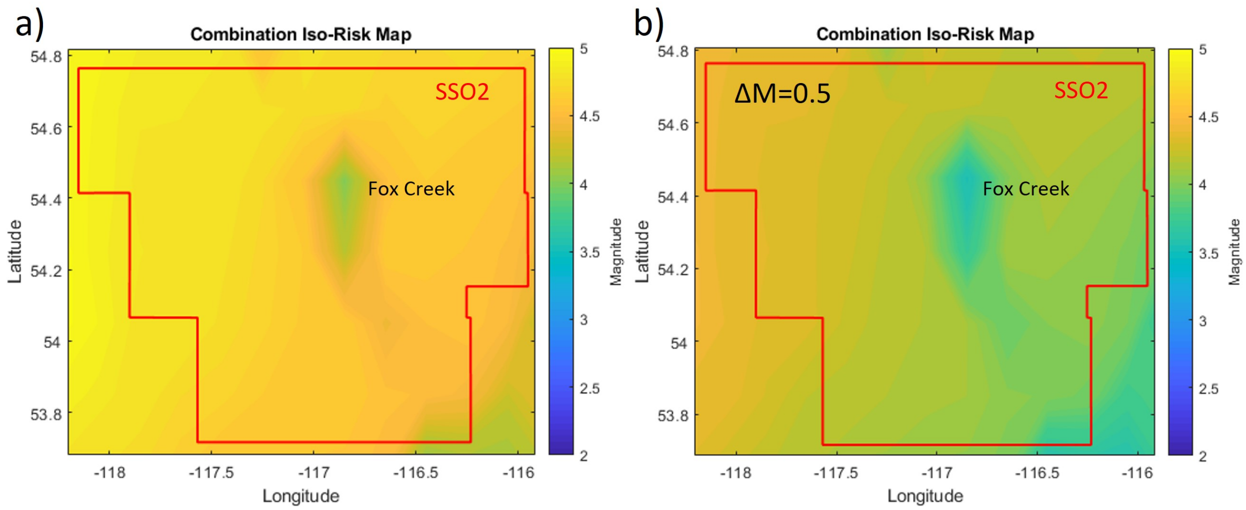

Figure 5. (a) Combination iso-risk map for the region defined by SSO2, using as tolerance levels 50% probability to cause nuisance to 30 000 households (CDI=3, equivalent to light-perceived shaking), and 50% probability to damage 3 households (DS=1, equivalent to slight/minor cosmetic damage). (b) Combination iso-risk map for the region defined by SSO2, subtracting a trailing seismicity factor of ΔM=0.5, and using the same tolerance levels as (a). Assuming this is an adequate trailing seismicity factor for hydraulic-fracturing activities, map (b) can be interpreted as a red-light map for hydraulic-fracturing activity. For reference, the figure shows the areas specified by SSO2.

5 Conclusion

We show a preliminary set of earthquake iso-nuisance, iso-damage, and combination iso-risk maps for Alberta, using different tolerance levels. By utilizing these maps, we can analyze the likelihood of nuisance and damage resulting from hypothetical earthquakes. This valuable information can aid in the effective management of induced seismicity, especially in cases involving newly induced seismic activity. Once the appropriate trailing seismicity factor is determined for a specific activity and location, these maps serve as the base for developing future red-light maps that will provide guidance for various industrial activities. Ongoing research includes a detailed analysis of the trailing seismicity to generate maps that can guide traffic light protocols for other anthropogenic seismicity cases in Alberta. When interpreting these maps, it is important to consider them as a conservative threshold for risk tolerance related to induced seismicity. Subsequent models could incorporate advanced frameworks for assessing human exposure that go beyond population distribution, such as critical infrastructure, potentially leading to different tolerance levels.

6 References

Alberta Energy Regulator (2015): Subsurface order no. 2; URL: https://static.aer.ca/prd/documents/orders/subsurface-orders/SO2.pdf [May 2023].

Alberta Energy Regulator (2019): Subsurface order no. 6; URL: https://static.aer.ca/prd/documents/orders/subsurface-orders/SO6.pdf [May 2023].

Alberta Energy Regulator (2019): Subsurface order no. 7; URL: https://static.aer.ca/prd/documents/orders/subsurface-orders/SO2.pdf [May 2023].

Alberta Energy Regulator (2021): Order under Sections 112 and 241 of the Environmental Protection and Enhancement Act (EPEA), ARC Resources Ltd. and Pembina Gas Services Ltd.; URL: https://www1.aer.ca/compliancedashboard/enforcement/202105-10_ARC%20Resources%20Ltd.%20and%20Pembina%20Gas%20Service%20Ltd._EPO.pdf [May 2023].

Atkinson, G.M., Eaton, D.W., Ghofrani, H., Walker, D., Cheadle, B., Schultz, R., Shcherbakov, R., Tiampo, K., Gu, J., Harrington, R.M., Liu, Y., van der Baan, M. and Kao, H. (2016): Hydraulic fracturing and seismicity in the Western Canada Sedimentary Basin; Seismological Research Letters, v. 87, p. 632–647.

Canadian Commission on Building and Fire Codes (2015): National Building Code of Canada 2015 Volume 1; National Research Council of Canada, Ottawa, NRCC 56190, 708 p.

Federal Emergency Management Agency (FEMA) (2015): Earthquake model Hazus-MH 2.1; *in* Multi-Hazard Loss Estimation Methodology Technical and User Manuals; URL: https://www.fema.gov/sites/default/files/2020-09/fema_hazus_earthquake-model_technical-manual_2.1.pdf.

Heath, D.C., Wald, D.J., Worden, C.B., Thompson, E.M. and Smoczyk, G.M. (2020): A global hybrid Vs30 map with a topographic slope–based default and regional map insets. Earthquake Spectra, v. 36, no. 3, p. 1570–1584.

Holzer, T.L., Padovani, A.C., Bennett, M.J., Noce, T.E. and Tinsley, J.C., III. (2005): Mapping NEHRP VS30 site classes; Earthquake Spectra, v. 21, no. 2, p. 353–370.

Pawley, S.M., Utting, D.J., Hartman, G., and Liggett, J.E. (2023): Thickness of sediments above bedrock and three-dimensional distribution of coarse-grained deposits in Alberta (gridded data, GeoTIFF format); Alberta Energy Regulator / Alberta Geological Survey, AER/AGS Digital Data 2023-0014.

Prior, G.J., Hathway, B., Glombick, P.M., Pana, D.I., Banks, C.J., Hay, D.C., Schneider, C.L., Grobe, M., Elgr, R. and Weiss, J.A. (2013): Bedrock geology of Alberta; Alberta Energy Regulator, AER/AGS Map 600.

Reyes Canales, M., Yusifbayov, J. and van der Baan, M. (2022): Evolution of short-term seismic hazard in Alberta, Canada, from induced and natural earthquakes: 2011–2020; Journal of Geophysical Research: Solid Earth, v. 127, e2021JB022822, https://doi.org/10.1029/2021JB022822.

Rose, A., McKee, J., Sims, K., Bright, E., Reith, A. and Urban, M. (2021): LandScan Global 2020 [Data set]. Oak Ridge National Laboratory, Oak Ridge, TN, USA.

Schultz, R. and Nanometrics Inc. (2019): Initial seismic hazard assessment for the induced earthquakes near Fox Creek, Alberta (between January 2013 and January 2016); Alberta Energy Regulator, Alberta Geological Survey, AER/AGS Special Report 104, 115 p.

Schultz, R., Beroza, G.C. and Ellsworth, W.L. (2021a): A risk-based approach for managing hydraulic fracturing–induced seismicity; Science, v. 372, no. 6541, p. 504–507.

Schultz, R., Beroza, G. C., & Ellsworth, W. L. (2021b). A strategy for choosing red-light thresholds to manage hydraulic fracturing induced seismicity in North America; Journal of Geophysical Research: Solid Earth, v. 126, no. 12, https://doi.org/10.1029/2021JB022340.

Schultz, R., Quitoriano, V. Wald, D.J. and Beroza, GC (2021c): Quantifying nuisance ground motion thresholds for induced earthquakes; Earthquake Spectra, v. 37(2), p. 789–802, https://doi.org/10.1177/8755293020988025.